

CLASSIFICATION OF FOCAL AND NON-FOCAL ELECTROENCEPHALOGRAM SIGNALS USING RECURRENCE PLOT METHODS

M.Tech. Thesis

By
KAPIL SWARNKAR



**DISCIPLINE OF ELECTRICAL ENGINEERING
INDIAN INSTITUTE OF TECHNOLOGY INDORE
JUNE 2016**

CLASSIFICATION OF FOCAL AND NON-FOCAL ELECTROENCEPHALOGRAPH SIGNALS USING RECURRENCE PLOT METHODS

A THESIS

*Submitted in partial fulfillment of the
requirements for the award of the
degree of*

Master of Technology
in

Electrical Engineering
with specialization in
Communication and Signal Processing

by

KAPIL SWARNKAR
(1402102006)



**DISCIPLINE OF ELECTRICAL ENGINEERING
INDIAN INSTITUTE OF TECHNOLOGY INDORE
JUNE 2016**



INDIAN INSTITUTE OF TECHNOLOGY INDORE

CANDIDATE'S DECLARATION

I hereby certify that the work which is being presented in the thesis entitled “**CLASSIFICATION OF FOCAL AND NON-FOCAL ELECTROENCEPHALOGRAM SIGNALS USING RECURRENCE PLOT METHODS**” in the partial fulfillment of the requirements for the award of the degree of **MASTER OF TECHNOLOGY** with specialization in **COMMUNICATION AND SIGNAL PROCESSING** and submitted in the **DISCIPLINE OF ELECTRICAL ENGINEERING** at **Indian Institute of Technology Indore**, is an authentic record of my own work carried out during the time period from **JULY 2015** to **JUNE 2016** under the supervision of **Dr. Ram Bilas Pachori**, Associate Professor of Electrical Engineering, IIT Indore.

The matter presented in this thesis has not been submitted by me for the award of any other degree of this or any other institute.

Signature of the student with date
(KAPIL SWARNKAR)

This is to certify that the above statement made by the candidate is correct to the best of my knowledge.

Signature of the Supervisor with date
DR. RAM BILAS PACHORI

KAPIL SWARNKAR has successfully given his M.Tech. Oral Examination held on **29-06-2016**.

Signature of Supervisor of M.Tech. thesis
Date:

Convener, DPGC
Date:

Signature of PSPC Member
Date:

Signature of PSPC Member
Date:

ACKNOWLEDGEMENTS

First of all, I would like to express my sincere gratitude to my thesis supervisor **Dr. Ram Bilas Pachori** for his constant support and guidance throughout this work.

I would also like to express my gratitude to my PSPC committee members Dr. Vivek Kanhangad and Dr. Anand Parey for their valuable suggestions.

I would also like to thank entire Department of Electrical Engineering for providing all the facilities and resources.

I would also like to thank all the faculty members of Electrical Engineering Department for teaching me during my course work which led to strong foundation for this work.

I would also like to thank Mr. Rajeev Sharma for his assistance at various stages of this work.

I am also thankful to all the members of Signal Analysis Lab for all their assistance.

I would also like to thank all the students of Electrical Engineering Research Lab for their help and guidance.

I would like to express my appreciation to my batch mates Anchal , Satyartha and Surabhi, for encouraging me through motivating and thoughtful discussions.

I am especially grateful to my family for their support and for believing in me.

KAPIL SWARNKAR

M.Tech. (Communication and Signal Processing)

Discipline of Electrical Engineering

IIT Indore

Dedicated
to
My Family

Abstract

The classification of focal and non-focal EEG signals is very useful for diagnosis of epilepsy. In this work, we propose a new approach for classifying focal and non-focal EEG signals using cross recurrence plot (CRP) and joint recurrence plot (JRP) methods. In our approach, EEG signals are decomposed into intrinsic mode functions (IMFs) using empirical mode decomposition (EMD) then CRP and JRP methods are applied on each IMF to form a feature vector. Finally, a binary classifier, least squares support vector machine (LS-SVM), is employed to discriminate focal and non-focal EEG signals. The proposed technique achieves 86% classification accuracy using CRP with linear and radial basis function (RBF) as kernels in LS-SVM classifier.

Contents

Abstract	i
1 Introduction	1
1.1 Types of epilepsy.....	1
1.1.1 Generalized epilepsy	1
1.1.2 Partial epilepsy.....	1
1.2 Electroencephalogram signals.....	2
1.2.1 Focal and non-focal EEG signals.....	2
1.3 Related work.....	3
1.4 Organization.....	4
2 Methodology.....	5
2.1 Dataset	6
2.2 Empirical mode decomposition.....	7
2.3 Recurrence plot.....	10
2.3.1 Phase space reconstruction.....	10
2.3.2 Recurrence plot structures.....	11
2.3.2.1 Single dots.....	11
2.3.2.2 Diagonal lines.....	11
2.3.2.3 Vertical or horizontal lines.....	11
2.3.3 Cross recurrence plot	11
2.3.4 Joint recurrence plot.....	14
2.4 Quantification analysis of recurrence plot.....	16
2.4.1 Parameters based on diagonals.....	17
2.4.1.1 Recurrence rate.....	17
2.4.1.2 Determinism.....	17
2.4.1.3 Average diagonal length	17

2.4.1.4 Recurrence times.....	18
2.4.1.5 Entropy.....	18
2.4.2 Parameters based on vertical lines.....	18
2.4.2.1 Laminarity.....	19
2.4.2.2 Trapping time.....	19
2.5 Least squares support vector machine.....	19
3. Results and Discussion.....	22
3.1 Results.....	22
3.2 Discussion.....	29
4 Conclusions and Future Work.....	31
4.1 Conclusions.....	31
4.2 Scope for future work.....	31
References.....	32

List of Figures

1.1 (a) Focal and (b) Non-focal EEG signal.....	2
2.1 Block diagram of proposed approach for classifying focal and non-focal EEG signals.....	5
2.2 Plot of “x” time series of EEG signal pairs: (a) Focal EEG signal, (b) Non-focal EEG signal.....	6
2.3 Plot of “y” time series of EEG signal pairs: (a) Focal EEG signal, (b) Non-focal EEG signal.....	7
2.4 Decomposition of focal EEG signals through EMD.....	9
2.5 Decomposition of non-focal EEG signals through EMD.....	9
2.6 Cross recurrence plot for focal EEG signals	13
2.7 Cross recurrence plot for non-focal EEG signals	14
2.8 Joint recurrence plot for focal EEG signals	15
2.9 Joint recurrence plot for non-focal EEG signals.....	16
3.1 Box plots for CRP parameters for without decomposition.....	27
3.2 Box plots for JRP parameters for without decomposition.....	27
3.3 Box plots for CRP parameters of IMF1.....	28
3.4 Box plots for JRP parameters of IMF1.....	28

List of Tables

3.1 p -values of features extracted from EEG signals and from different IMFs by CRP method.....	23
3.2 p -values of features extracted from EEG signals and from different IMFs by JRP method.....	24
3.3 Comparison of classification accuracy of CRP and JRP methods.....	25
3.4 Comparison of classification accuracy obtained from the different classification methods	29

Chapter 1

Introduction

Epilepsy [1, 2, 3] is one of the most widely recognized neurological disorders that causes seizures. Epilepsy may occur because of sickness, cerebrum damage, or unusual advancement of brain [1]. At present, the estimated extent of the overall population with active epilepsy is somewhere around 4 to 10 people for every 1,000 individuals [4]. However, according to some studies of developing nations indicates that the extent to which people are affected by epilepsy is somewhere around 7 to 14 for every 1000 people [4]. Nearly 80% of epilepsy cases are found in developing nations [4]. Approximately 20% patients have generalized epilepsy and 60% patients have focal or partial epilepsy [1]. In order to surgical treatment of the epilepsy, identification of the brain area which have epileptic seizure becomes a very important step and there are various non-linear methods that can be used for the identification of the epileptic brain area.

1.1 Types of epilepsy

The epilepsy can be broadly classified as in two categories [5]

1. Generalized epilepsy
2. Partial epilepsy

1.1.1 Generalized epilepsy

In this class of epilepsy, seizures have their effect over entire brain [5].

1.1.2 Partial epilepsy

This kind of epilepsy, seizures start in limited part of the brain [5]. It can be treated by surgical resection of responsible brain area.

1.2 Electroencephalogram signals

An electroencephalogram (EEG) [6, 7, 8] is a signal that depicts the electrical activities of the brain. Various frequency components are present in EEG signals that make the EEG signals complex in nature. These signals represent how human brain works and contain information related to the neurological disorder. Therefore EEG signals can be used for assessment of these disorders. There are some disorders that may occur due to repetitive discharge from the cerebral cortex and lead to malfunctioning of the brain. Such type of disorders are grouped as the epileptic seizure. Detection of epilepsy is very important because it affects the normal life condition of a patient. The focal (S_{focal}) and non-focal ($S_{nonfocal}$) EEG signals [9, 10, 11, 12] can be useful for identification of brain area affected by epilepsy. Brief overview of these signals is as follows.

1.2.1 Focal and non-focal EEG signals

The S_{focal} and $S_{nonfocal}$ EEG signals are obtained from the patients influenced by partial or focal epilepsy [9]. Partial epilepsy influences just a limited part of the brain. The S_{focal} EEG signals are those EEG signals which are obtained from the channels where epileptic seizures are observed. The $S_{nonfocal}$ EEG signals are obtained from the remaining channels where the epileptic seizure is not observed. Figure 1.1 shows the S_{focal} and $S_{nonfocal}$ EEG signals respectively which are taken from Bern Barcelona database [9].

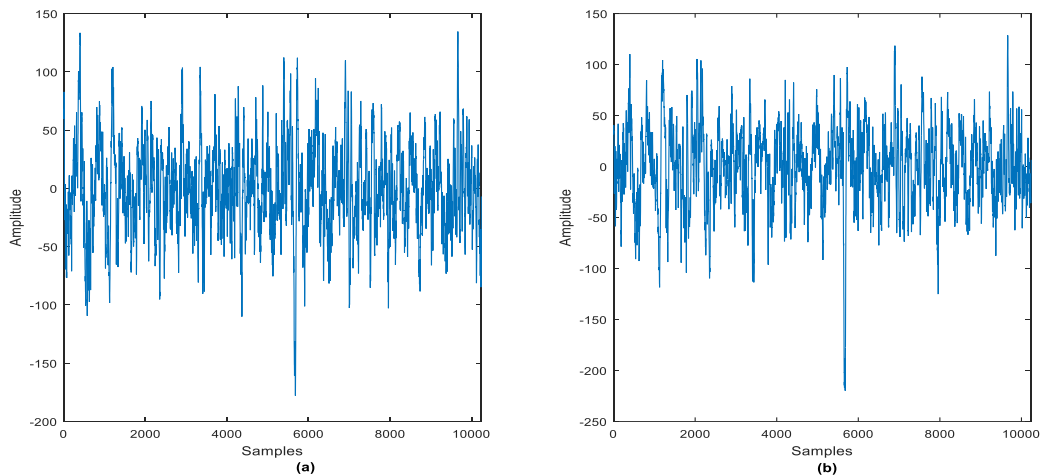


Figure 1.1: (a) Focal and (b) Non-focal EEG signal

1.3 Related work

The characteristics of part of brain which is responsible for epilepsy (epileptogenic focus) can be studied using different nonlinear parameters. Recently, various nonlinear parameters are used to analysed EEG signals in order to characterise the epileptogenic focus. In the existing literature, approximate entropy [13], correlation dimension [14], phase synchronization along with surrogate analysis [15], coherence patterns [16], the time-variant connectivity measure and modified effective connectivity measure [17], moving window correlation dimension [18], etc. are analysed to learn about epilepsy related dynamics of brain. The concluding remarks obtained from above studies depict that non-linear parameters can be helpful for the localization of epileptogenic focus as well as these are useful in the representation of non-linear brain dynamics.

The S_{focal} EEG signals are intracranial recordings obtained from patients with partial epilepsy and can be useful to characterise the epileptogenic focus [12]. Therefore, the classification of S_{focal} and S_{nonfocal} EEG signals can be useful for identification of epileptogenic focus. Recently, a technique based on empirical mode decomposition (EMD) [19] has been proposed for the classification of S_{focal} and S_{nonfocal} EEG signals [10, 12]. EMD is used to decompose a signal into various modes termed as intrinsic mode functions (IMFs) [19, 20, 21]. These IMFs are used to derive different features used to study epileptic seizures. Discrete wavelet transform (DWT) [11] based features also used to classify EEG signals into focal and non-focal categories. In DWT based approach, entropies (from the energies of detail coefficient) such as Shannon wavelet entropy (S_e), Tsallis wavelet entropy (T_e) and Renyi wavelet entropy (R_e) are computed and further averaged to be used as a feature [11]. These entropies are employed as the input features for different classifiers. The various features are prioritize using different feature ranking methods [11].

In the present work, we analysed the EEG signals using recurrence plot (RP) analysis and presented a new method based on features extracted using RP for the classification of S_{focal} and S_{nonfocal} EEG signals. First, we obtained the recurrence plot from the given data and then some parameters namely recurrence rate, entropy, maxline, trapping time, laminarity are evaluated from that plot. The above mentioned RP based features are computed in two cases, first directly from the EEG signals, and in the second case from the IMFs obtained by applying EMD method on EEG signals. These evaluated parameters are employed as the input features for classifiers. Before classification

some feature ranking methods are used to prioritize and reducing complexity of the classification system. We have compared the results obtained in terms of classification accuracy for both the mentioned cases.

1.4 Organization

The rest of the thesis is organised as: A detailed description of the proposed methodology is presented in chapter 2, which includes brief review of EMD, recurrence plot (RP), cross recurrence plot (CRP), joint recurrence plot (JRP), parameters used for recurrence quantification analysis, and least squares support vector machine (LS-SVM). Chapter 3 presents experimental results, and concluding remarks are given in chapter 4.

Chapter 2

Methodology

The classification of S_{focal} and $S_{nonfocal}$ EEG signals is carried out in four steps. Firstly, EMD method [19] is used for finding the various IMFs of EEG signals. Then, recurrence quantification analysis based on CRP and JRP [22] is performed for extracting features from the S_{focal} and $S_{nonfocal}$ EEG signals and their IMFs. This is followed by ranking of these features. Finally, based on the features obtained, the LS-SVM [23] classifies the signals into S_{focal} and $S_{nonfocal}$ EEG signals. The block diagram of the proposed methodology is shown in Figure 2.1.

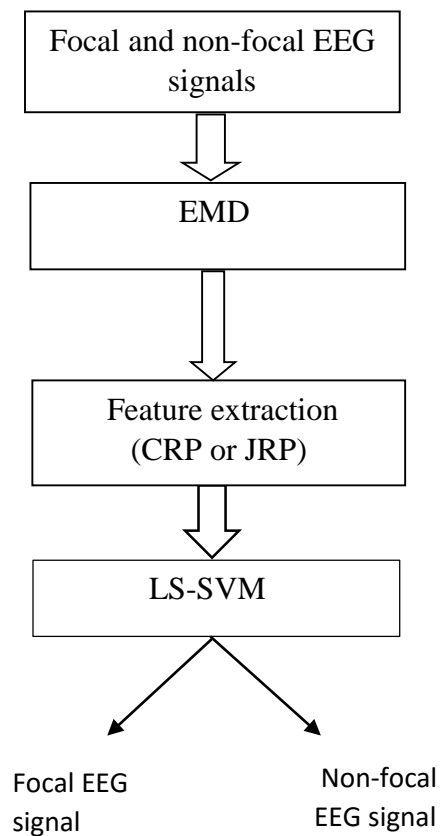


Figure 2.1: Block diagram of proposed approach for classifying focal and non-focal EEG signals.

2.1 Dataset

The dataset for S_{focal} and S_{nonfocal} EEG signals are downloaded from Bern Barcelona database (www.dtic.upf.edu/~ralph/sc/) [9]. The dataset contains the bivariate recordings of S_{focal} and S_{nonfocal} EEG signals. The recordings acquired from the five patients affected by temporal lobe partial epilepsy [9]. The signals have been measured in seizure-free intervals. The two time series of the bivariate EEG signals are represented by symbols “x” and “y”. The duration of each EEG signal is 20 seconds and sampling frequency is 512 Hz. There are 3750 pairs of EEG signals for both categories of EEG signals. In this work, a small subset has been formed by taking the 50 pairs of S_{focal} and 50 pairs of S_{nonfocal} EEG signals. This small subset has been used for further experiments. Figure 2.2 depicts plot of “x” time series of a S_{focal} and a S_{nonfocal} EEG signals. Similarly, Figure 2.3 depicts plot of “y” time series of a S_{focal} and a S_{nonfocal} EEG signals.

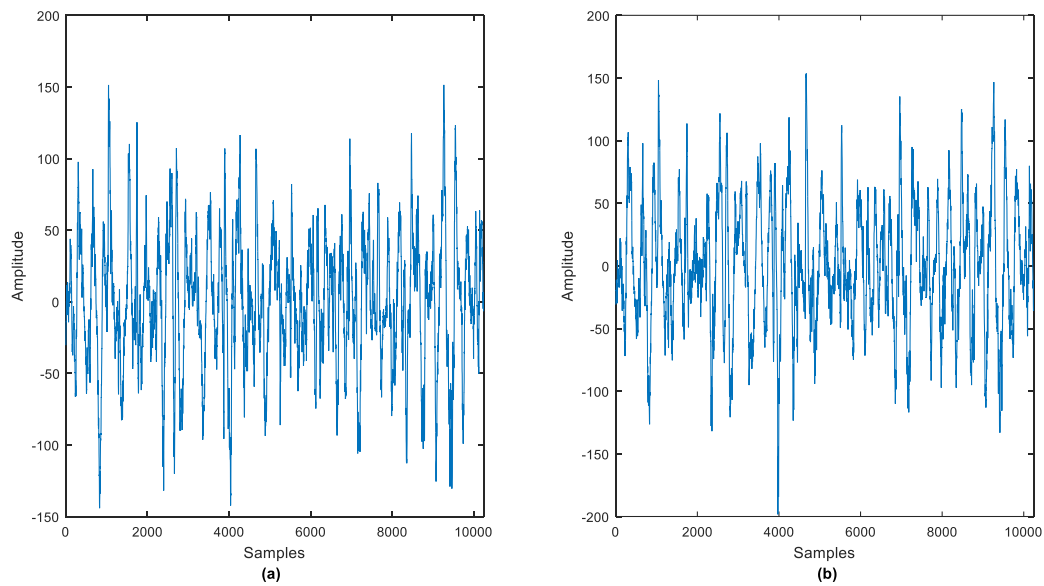


Figure 2.2: Plot of “x” time series of EEG signal pairs: (a) Focal EEG signal, (b) Non-focal EEG signal.

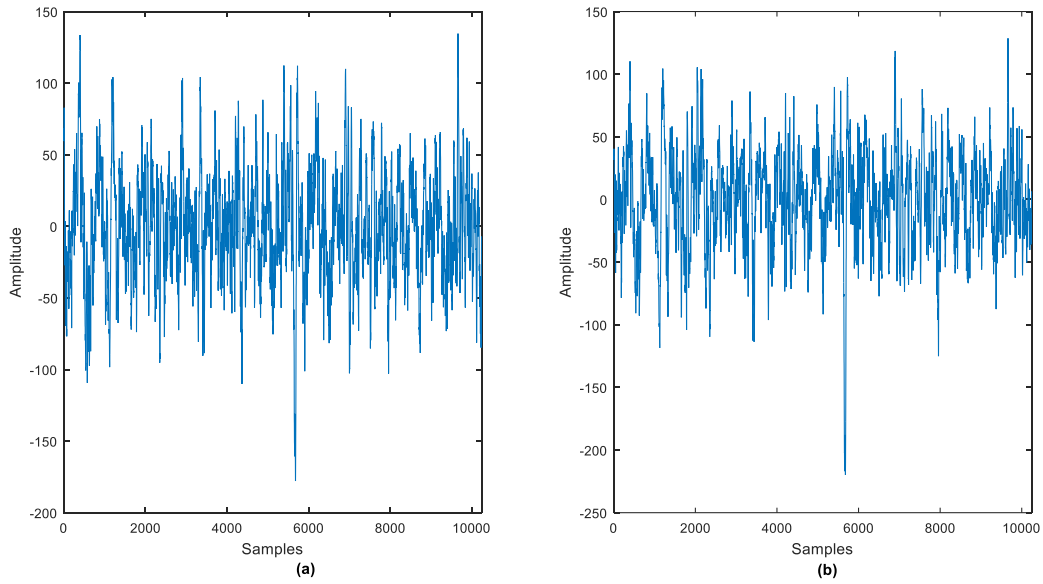


Figure 2.3: Plot of “y” time series of EEG signal pairs: (a) Focal EEG signal, (b) Non-focal EEG signal.

2.2 Empirical mode decomposition

The EMD method [19] decomposes a signal into different modes known as intrinsic mode functions (IMFs). The IMFs are oscillatory signals which can be considered frequency as well as amplitude modulated [24]. In this decomposition, no condition is required on the signals like linearity and stationarity.

An IMF, obtained as a result of decomposition of EEG signals using EMD, must satisfy the below mentioned basic conditions [19, 25, 26]:

1. The total number of minima and maxima and the total number of zero-crossings should either be equal or at most differ by one.
2. The average value of the envelopes, which are obtained using local minima and maxima, should be zero at all the sample instants.

For a signal $x(t)$ sifting process can be summarized as follows [19]:

1. Let $h(t) = x(t)$.
2. Extrema are obtained from $h(t)$.
3. Evaluate lower envelope $e_l(t)$ and upper envelope $e_u(t)$ by connecting minima and maxima respectively.
4. Evaluate mean envelope $e_m(t)$ by averaging $e_u(t)$ and $e_l(t)$, as

$$e_m(t) = \frac{e_u(t) + e_l(t)}{2} .$$

5. Subtracting $e_m(t)$ from signal $h(t)$ as $h_1(t) = h(t) - e_m(t)$.
6. Impose the IMFs conditions on $h_1(t)$ and examine whether IMF is a valid IMF or not.
7. Repeat steps 2 to 6, until $h_1(t)$ is found to be valid IMF.

On obtaining the valid IMF, assign $D_1(t) = h_1(t)$. Further we get $r(t)$ after applying $r(t) = x(t) - D_1(t)$. Then, $x(t)$ is replaced with $r(t)$ i.e. $x(t) = r(t)$. For obtaining the next IMF, again steps 2 to 7 are repeated by posing $h_1(t) = r(t)$. Consequently, $x(t)$ is given as [19]

$$x(t) = \sum_{i=1}^M D_i(t) + r(t) \tag{2.1}$$

Here, M denotes the number of the IMFs in $x(t)$ and $r(t)$ represents the residual of $x(t)$. Figure 2.4 depicts the extracted IMFs from “x” time series of S_{focal} EEG signal which is shown in Figure 2.2. In a similar way, Figure 2.5 depicts the extracted IMFs from “x” time series of S_{nonfocal} EEG signal which is shown in Figure 2.2.

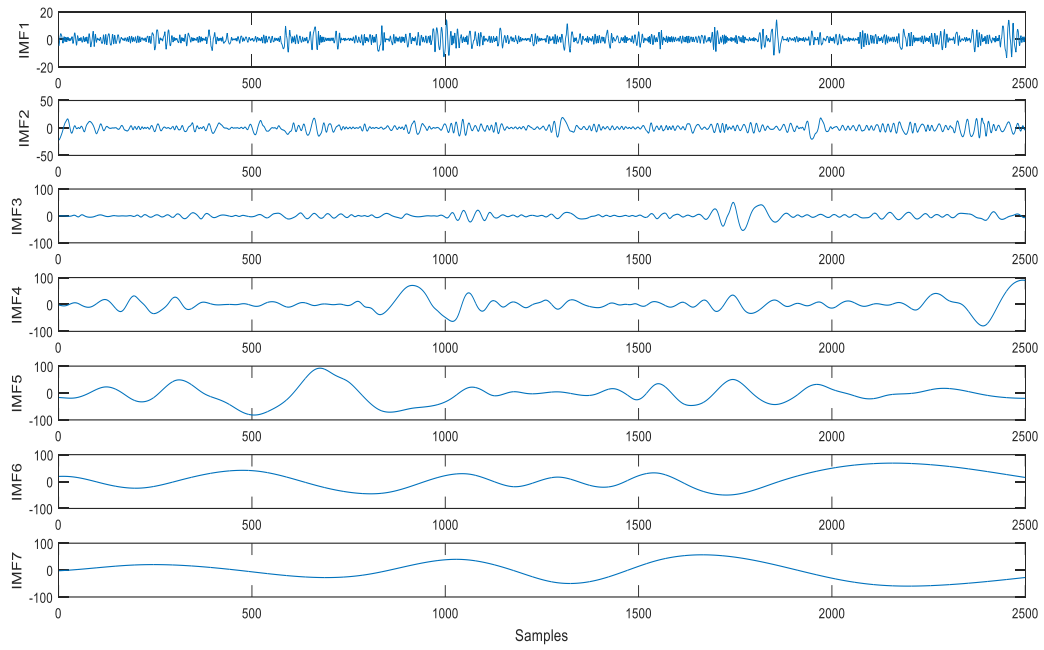


Figure 2.4: Decomposition of focal EEG signals through EMD

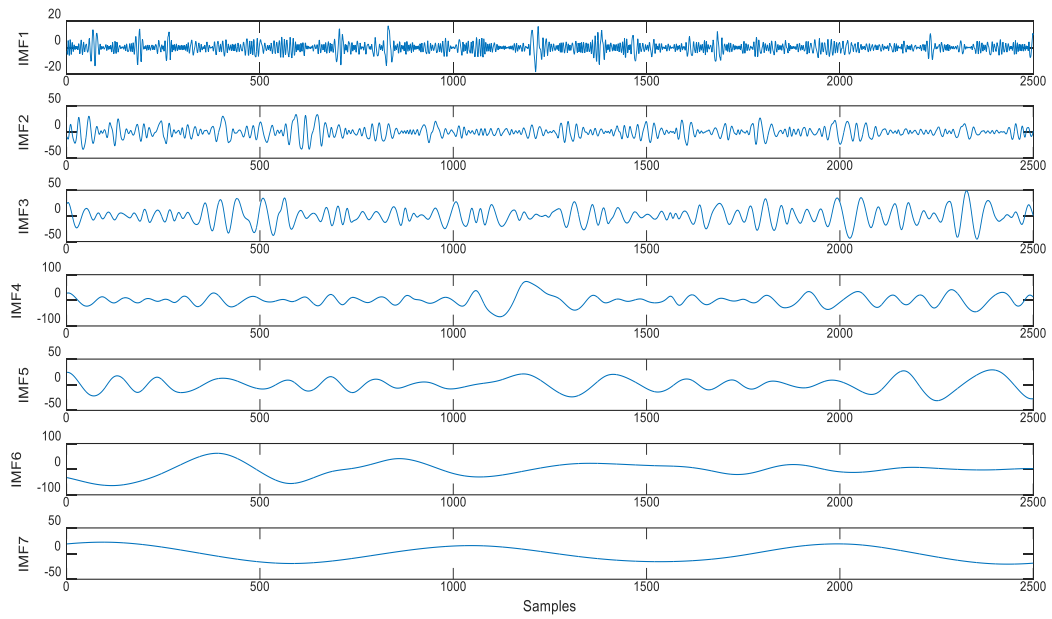


Figure 2.5: Decomposition of non-focal EEG signals through EMD

2.3 Recurrence plot

RP [22, 27, 28] is a very basic tool designed for analysing the repetitive nature of dynamic systems. It is also suited for non-linear analysis of signals that is of short duration and has non-stationary characteristics.

Recurrence quantification analysis can be describe in the following steps [22, 27]:

Step 1: Reconstruction of phase space

Step 2: Recurrence plot formation with threshold distance

Step 3: Evaluation of measures for recurrence plot

RP represents all the trajectories of phase space for a non-linear system [22]. A trajectory depicts all the states that can exist for a system and every state relates to a particular point in the phase space.

2.3.1 Phase space reconstruction

The RP is a graphical representation of the phase space trajectories of any non-linear system [22]. Trajectories in phase space represent all possible states of a system. Each state of the system corresponds to a specific point in the phase space. For any system, the phase space trajectory $X(t)$ can be reconstructed from the time series $x(t)$ using Taken's embedding theorem [29], as described below:

$$X_i = (x_i, x_{i+\beta}, \dots, x_{i+(n-1)\beta}) \quad (2.2)$$

where β is time delay, n is embedding dimension. False nearest neighbour method [30] is used for evaluating 'n' and mutual information method [30] is used for evaluating the value of ' β '. An optimal set of embedding dimension and time delay is important for reconstruction of phase space that fully describes the system dynamics.

Then the recurrence plot is obtained from the equation given below [22].

$$Z_{i,j}(\tau) = \Theta(\epsilon - \|x_i - x_j\|) \quad (2.4)$$

Where, ϵ is threshold value, $\|\cdot\|$ is norm and $\Theta(x)$ represents Heaviside function. The most important parameter of recurrence analysis is the threshold. If the distance between two states on

the phase space trajectory is smaller than a given threshold, then the recurrence point in RP arises. Value of the point in recurrence matrix is either one or it is zero.

2.3.2 Recurrence plot structures

A closer examination of the RP represents the small-scale structures, which may be generally classified in diagonal lines, dots, and vertical or horizontal lines [22].

2.3.2.1 Single dots

Single dots [22] on the RP indicates a single state, repeating rarely. Such states persist only for a short time period in phase space.

2.3.2.2 Diagonal lines

A diagonal line (D_l) occurs on RP when a point $Z_{i+k,j+k} = 1$ for different values of k varying from 1 to $l-1$ (where l = diagonal length). In the phase space, whenever segment of trajectory runs parallel to another segment form a diagonal line in RP. A diagonal line is defined by [22]

$$(1-Z_{i-1,j-1}) (1-Z_{i+l,j+l}) \prod_{k=0}^{l-1} Z_{i+k,j+k}=1. \quad (2.5)$$

2.3.2.3 Vertical or horizontal lines

A vertical line (D_v) occurs on RP when a point $Z_{i,j+k} = 1$ for different values of k varying from 1 to $v-1$ (where v = length of vertical line). It represents a constant state of the time series. A vertical line is then defined by [22]

$$(1-Z_{i-1,j-1}) (1-Z_{i+v,j+v}) \prod_{k=0}^{v-1} Z_{i+k,j+k}=1 \quad (2.6)$$

2.3.3 Cross recurrence plot

The bivariate expansion of RP is known as cross recurrence plot (CRP) [22, 31, 32] which is the generalization of linear cross-correlation function. Similar to RP, the structure of CRP have dots, diagonal lines and vertical or horizontal lines.

Assume that x_i and y_j represents the states corresponding to two different dynamical systems. Then, similar to the Recurrence Plot, the CRP is defined by [22]

$$X_{i,j}(\epsilon) = \theta(\epsilon - \|x_i - y_j\|) \quad (2.7)$$

where i and j take values as $i = 1,2,3 \dots N$, and $j = 1,2,3 \dots M$.

The CRP shows valuable information about the relationship between two time series where the diagonal line which have long length show similar phase space nature of both systems and distorted diagonal line shows different nature of both time series [22].

In the CRP, it is not necessary to have the main diagonal with all elements equal to one and therefore, in Figure 2.6-2.7 main diagonal is not present. Moreover, the structures that are presents in RP are as well present in CRP. The lines that have their orientation with diagonal play an important role in the analysis. These depict the segments on both the trajectories that are parallel for some duration. The length and frequency of the above lines tells the similarity between the dynamic behaviour of both systems. The length based measure can be helpful in finding the non-linear inter-relations between the two systems that is not possible through the common cross-correlation function.

Figure 2.6 depicts cross recurrence plot for “x” and “y” time series of a S_{focal} EEG signal. Similarly, Figure 2.7 depicts cross recurrence plot for “x” and “y” time series of S_{nonfocal} EEG signals.

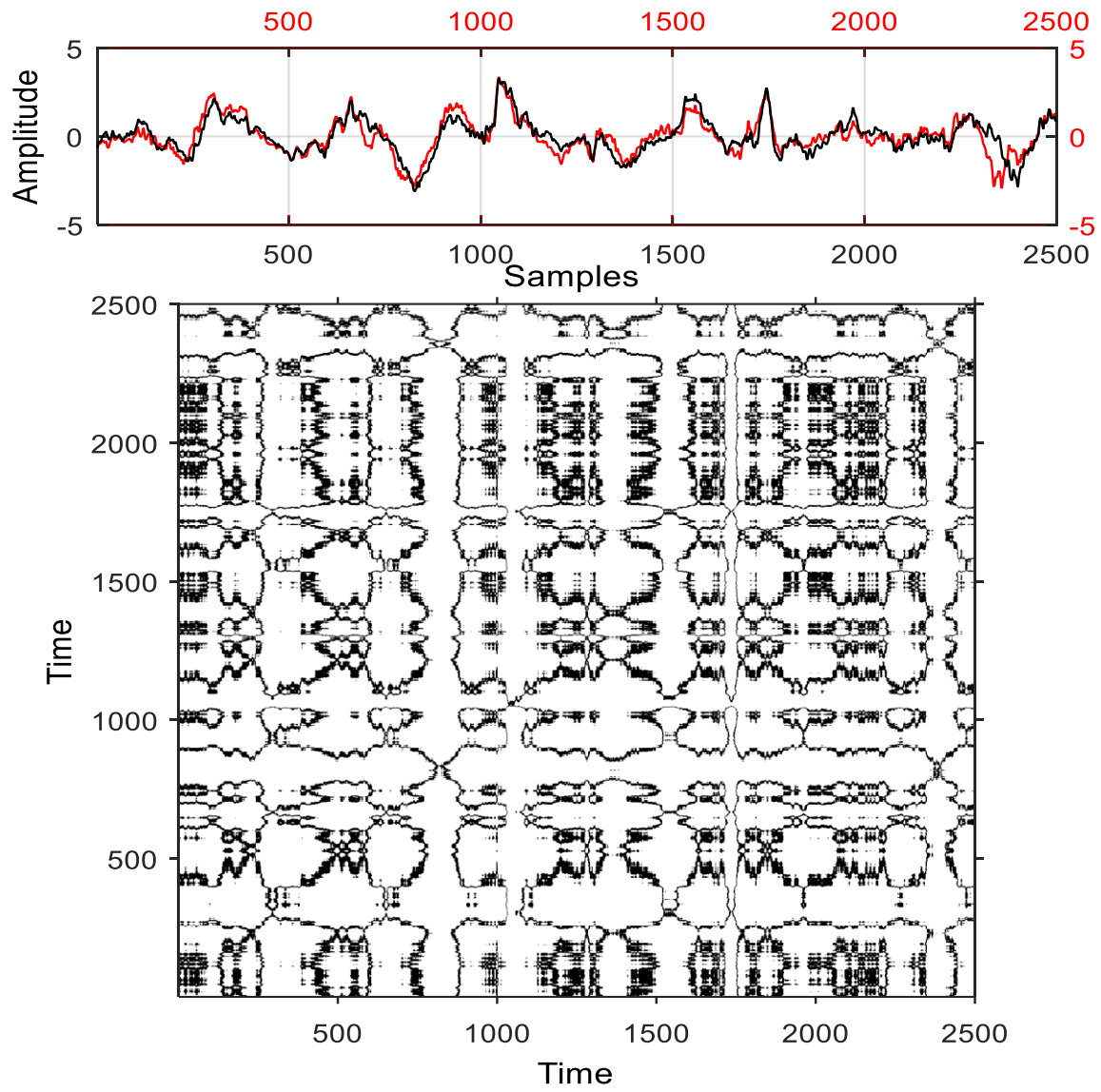


Figure 2.6: Cross recurrence plot for focal EEG signals

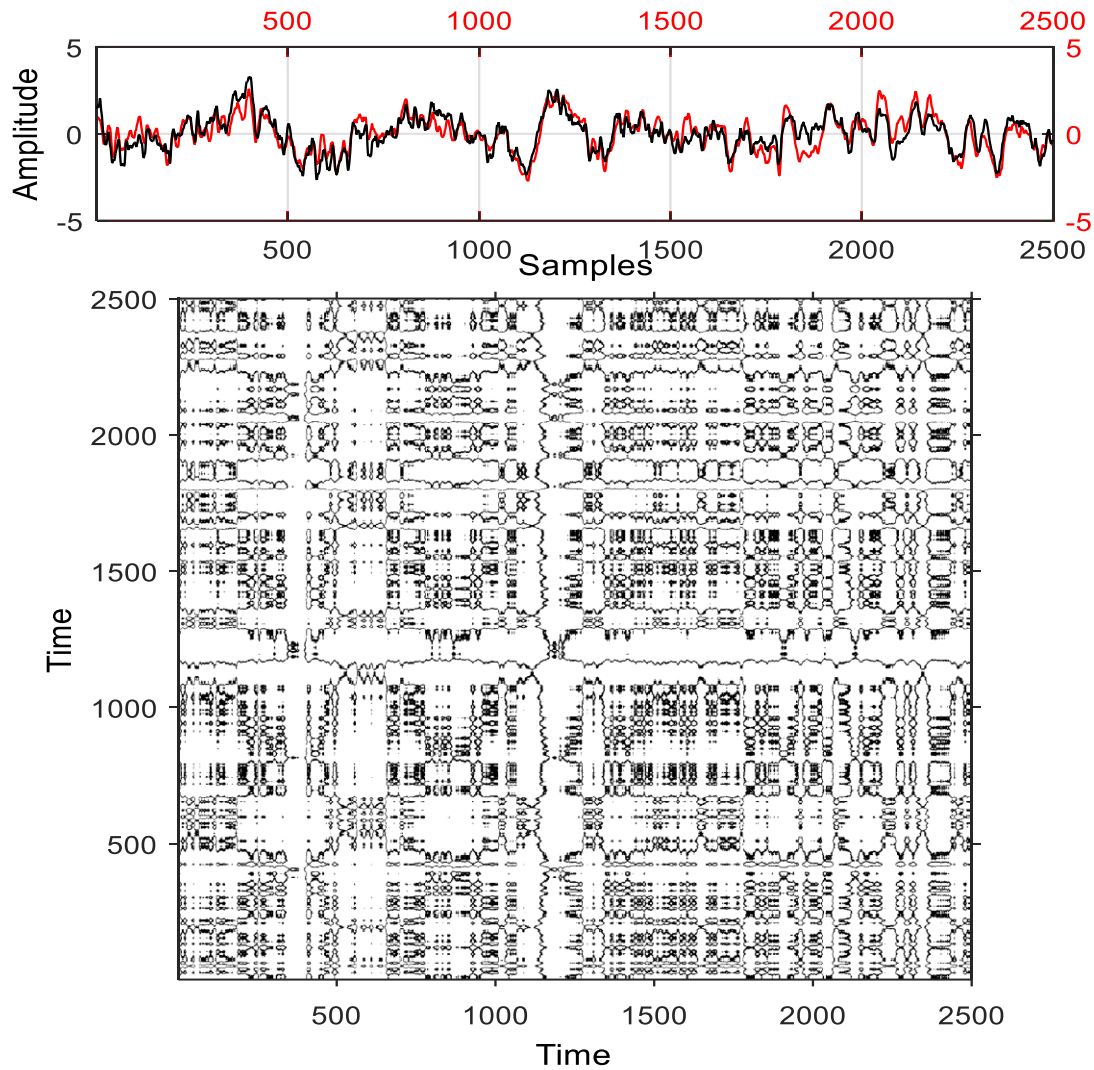


Figure 2.7: Cross recurrence plot for non-focal EEG signals

2.3.4 Joint recurrence plot

It is different approach to compare the two systems is through joint recurrence plot [22]. The recurrences of trajectories for both the systems are studied separately in individual phase spaces. The instants when both the systems recur simultaneously are noted. Using this approach, the phase spaces are not affected and it gives rise to the extended phase space denoted as $R(dx + dy)$, where

dx and dy are the phase space dimensions of the corresponding systems. The joint recurrence matrix for two systems $x(t)$ and $y(t)$ is given by [22]

$$JR_{i,j} = \theta(\epsilon - \|x_i - x_j\|) \theta(\epsilon - \|y_i - y_j\|) \quad (2.8)$$

$$i, j = 1, 2, 3 \dots N$$

Figure 2.8 depicts joint recurrence plot for “x” and “y” time series of a S_{focal} EEG signal. Similarly, Figure 2.9 depicts joint recurrence plot for “x” and “y” time series of S_{nonfocal} EEG signals.

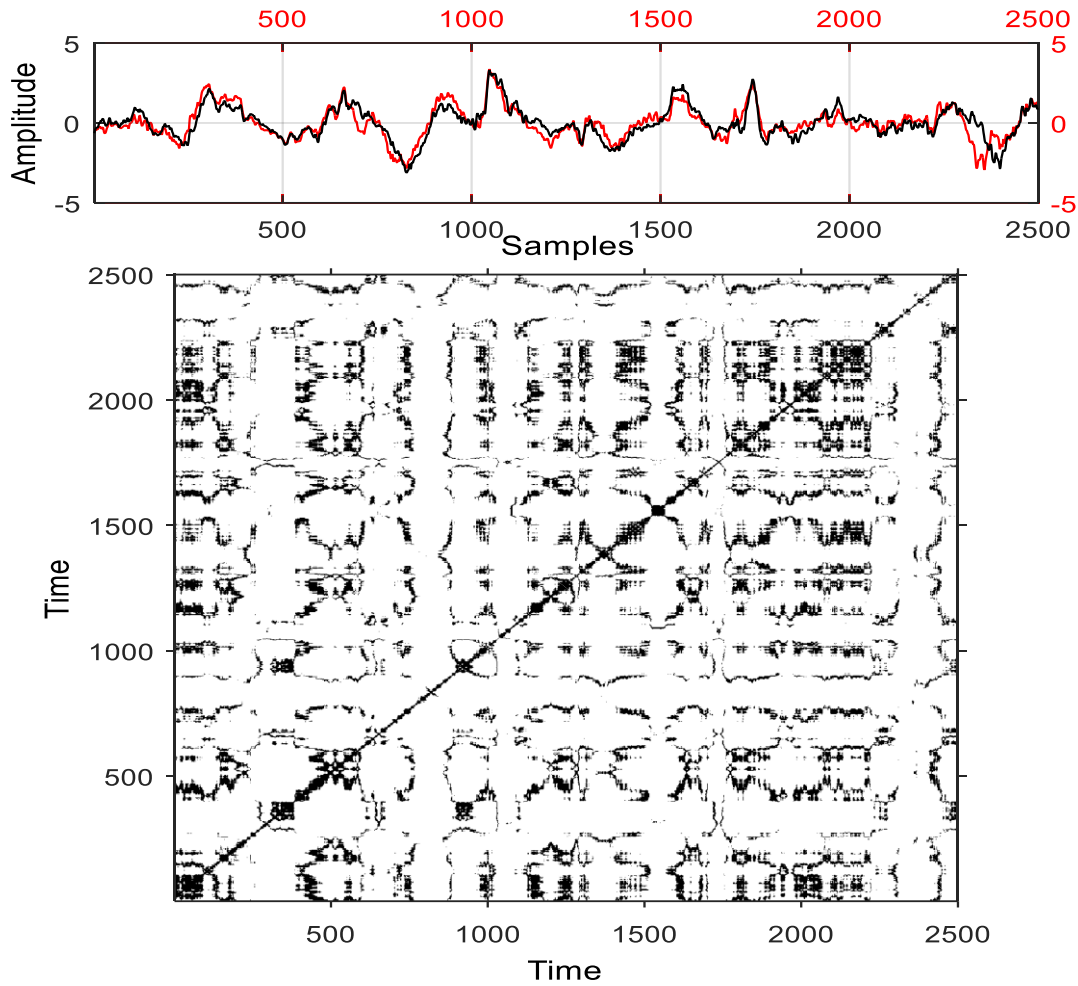


Figure 2.8: Joint recurrence plot for focal EEG signals

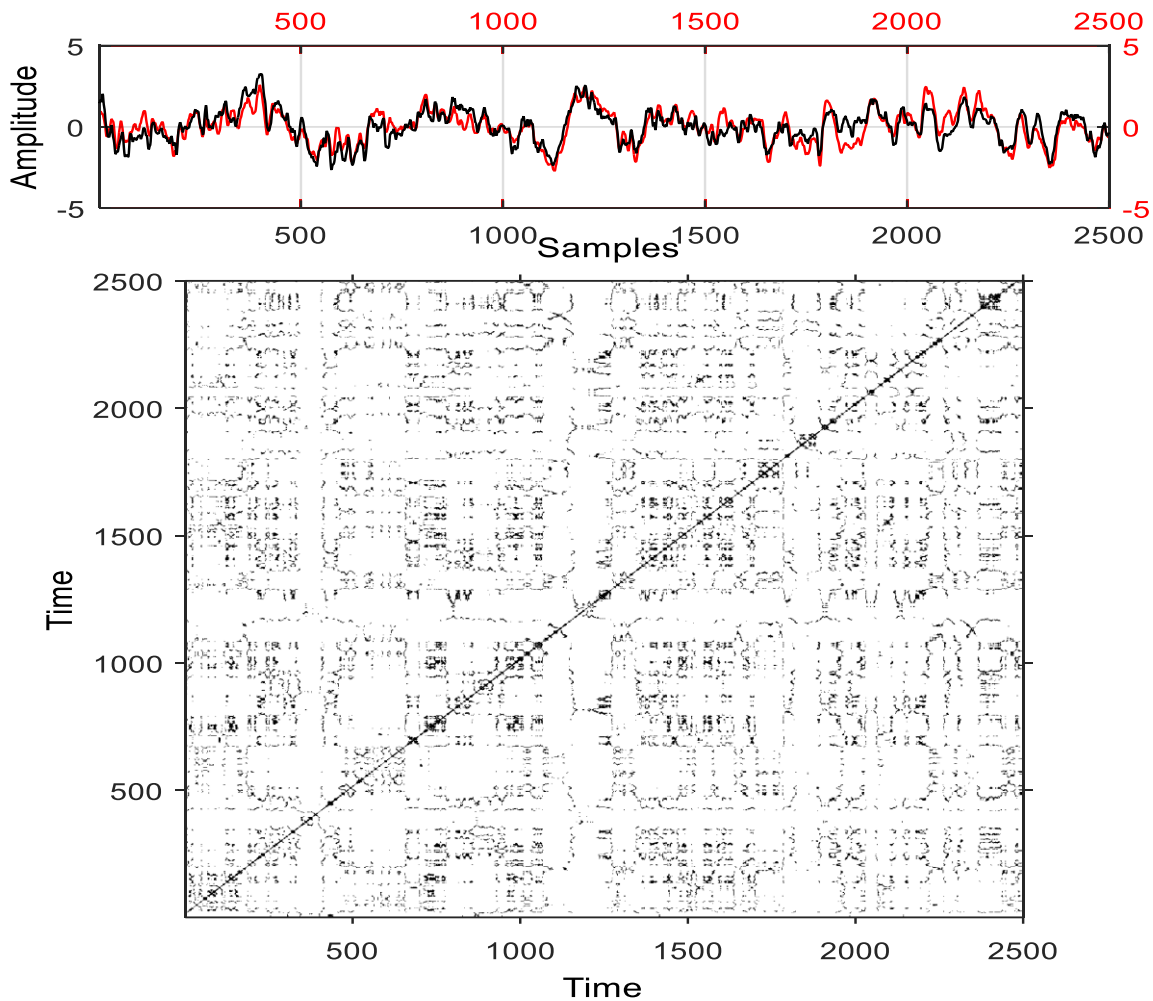


Figure 2.9: Joint recurrence plot for non-focal EEG signals

2.4 Quantification analysis of recurrence plot

Recurrence quantification analysis (RQA) [33, 34, 35] is used to find the useful parameters from the CRP and JRP. These parameters are used as input features for the classifier.

2.4.1 Parameters based on diagonals

The parameters namely recurrence rate, determinism, average diagonal length, recurrence times and entropy are based on diagonal line parameters of RP. These parameters are briefly explained as follows [22]:

2.4.1.1 Recurrence rate

Recurrence rate (RR) is density of recurrence points of RP where point (i, j) repeats if the separation between the vectors x_i and y_j is less than the threshold. Equation 2.9 [22] is used to evaluate the value of RR.

$$RR(\epsilon) = \frac{1}{N^2} \sum_{i,j=1}^N Z_{i,j} \quad (2.9)$$

2.4.1.2 Determinism

Determinism (DET) [22] is the percentage of repetitive points of RP. These points represent the line segments parallel to the primary diagonal and shows the deterministic structure. It is defined by [22]

$$DET = \frac{\sum_{l=lmin}^N lP(l)}{\sum_{l=1}^N lP(l)} \quad (2.10)$$

where $P(l)$ is the frequency distribution of diagonal lines which is defined by [22].

$$P(l) = \sum_{i,j=1}^l (1 - Z_{i-1,j-1}) (1 - Z_{i+l,j+l}) \prod_{k=0}^{l-1} Z_{i+k,j+k}$$

where l is the length of diagonal line.

2.4.1.3 Average diagonal length

The average diagonal length (ADL) is the average value of all diagonals which are parallel to primary diagonals of RP [22, 35]. It is calculated by the equation 2.11 [22]

$$ADL = \frac{\sum_{l=lmin}^N lP(l)}{\sum_{l=lmin}^N P(l)} \quad (2.11)$$

where $P(l)$ is the frequency distribution of diagonal lines and l is the length of diagonal line.

2.4.1.4 Recurrence times

The time at which the point is recur is known as recurrence times (RT). 1^s t and 2nd poicare recurrence points are given by [22]

$$RT = t_{i+1} - t_i, \quad t = 1, 2, \dots K \quad (2.12)$$

$$RT2 = t_{j+1} - t_j, \quad t = 1, 2, \dots K$$

2.4.1.5 Entropy

The entropy (ENTR) is the distribution of the line segments that are parallel to the primary diagonal. The entropy indicates, the amount of data are required to reconstruct the system. A low entropy shows that lower information is required to recognize the system, and a high entropy demonstrates that higher information are required for the system recognition. The entropy is low when the length of longest line (parallel to the diagonal) is short and does not differ much. It is calculated by the equation given below [22]

$$ENTR = - \sum_{l=lmin}^N P(l) \ln P(l) . \quad (2.13)$$

where $P(l)$ is the frequency distribution of diagonal lines and l is the length of diagonal line

2.4.2 Parameters based on vertical lines

Laminarity and trapping time (TT) parameters are based on vertical line parameters. These parameters are explained as follows [22]

2.4.2.1 Laminarity

Laminarity (LAM) is the amount of recurrence points which form vertical line. It quantifies the amount of laminar states. It is evaluated by following equation [22]:

$$\text{LAM} = \frac{\sum_{v=v_{\min}}^N vP(v)}{\sum_{v=1}^N vP(v)} \quad (2.14)$$

where $P(v)$ is the frequency distribution of vertical lines which is defined as

$$P(v) = \sum_{i,j=1}^v (1 - Z_{i-1,j-1}) (1 - Z_{i+v,j+v})$$

where v is the length of vertical line.

2.4.2.2 Trapping time

The normal length of vertical structures is given by the trapping time (TT). Which is calculated by the following equation [22]:

$$\text{TT} = \frac{\sum_{v=v_{\min}}^N vP(v)}{\sum_{v=v_{\min}}^N P(v)} \quad (2.15)$$

where $P(v)$ is the frequency distribution of vertical line and v is the length of vertical line.

2.5 Least squares support vector machine

Support vector machine (SVM) [36, 37] is used for classification of input data by constructing optimal hyperplane. Optimal hyperplane maximizes the distance between two data points that are nearest and belong to two different classes. It is based on statistical learning theory. To classify the data, SVM constructs optimal separating hyperplane which maximizes the separation between the two nearest data points which belongs to two different classes. Consider N number of data points $\{x_i, y_i\}_{i=1}^N$, where $x_i \in \mathbb{R}$ is input and $y_i \in \{+1, -1\}$ is class label. For classification problem having two classes, hyperplane that separates these points is given as [37, 38]

$$F(x) = \text{sign}[\Omega^T g(x) + \beta] \quad (2.16)$$

where Ω is weight vector of dimension d and $g(x)$ is a function that maps data point x into the given d -dimensional space and the bias value is taken as β . The version of SVM that uses least squares algorithm is known as least squares support vector machine (LS-SVM). The problem of classification using the above mentioned method can be formulated as [37]:

$$\min_{\Omega, \beta, \epsilon} J(\Omega, \beta, \epsilon) = \frac{1}{2} \Omega^T \Omega + \frac{\gamma}{2} \sum_{i=1}^N \epsilon_i^2 \quad (2.17)$$

subjected to the following equality constraint

$$y_i [\Omega^T g(x_i) + \beta] = 1 - \epsilon_i \quad i = 1, 2, 3, \dots, N \quad (2.18)$$

where $\epsilon_i = (\epsilon_1, \epsilon_2, \epsilon_3, \dots, \epsilon_N)^T$.

The Lagrangian multiplier α_i for (2.17) can be defined as [37]:

$$L(\Omega, \beta, \epsilon, \alpha) = j(\Omega, \beta, \epsilon) - \sum_{i=1}^N \alpha_i \{y_i [\Omega^T g(x_i) + \beta] - 1 + \epsilon_i\} \quad (2.19)$$

On solving (2.19) by considering the optimal conditions, LS-SVM classifier is calculated as [37, 12]

$$f(x) = \text{sign}(\sum_{i=1}^N \alpha_i y_i H(x, x_i) + \beta) \quad (2.20)$$

where $H(x, x_i)$ is a kernel function. In the presented work, different kernel functions have been used whose definitions are given as follows:

1. Linear kernel function [39]:

$$H(x, x_i) = x \cdot x_i$$

2. Polynomial kernel function [40]:

$$H(x, x_i) = (x \cdot x_i + 1)^d$$

where d is the polynomial degree.

3. Radial basis function kernel [40]:

$$H(x, x_i) = e^{-\frac{\|x-x_i\|^2}{2\sigma^2}}$$

where σ controls the Radial basis function kernel function width.

Chapter 3

Results and Discussion

In this chapter, we present the experimental results and discussion based on the proposed methodology which has been explained in previous chapter.

3.1 Results

We have performed the recurrence quantification analysis for the classification of S_{focal} and S_{nonfocal} EEG signals, basically this analysis is based on CRP and JRP methods. We apply these methods on the signals without decomposition and on the different IMFs obtained using the EMD method. Wilcoxon test [41, 11], Bhattacharya test [42, 11] and ROC test [43, 11] are used for the ranking the different features. The initial 2500 samples are taken from each signal for the analysis. The CRP and JRP parameters have been computed for initial seven IMFs and these parameters are used as features for classification of S_{focal} and S_{nonfocal} EEG signals. Discrimination performance has been evaluated and quantified using Kruskal-Wallis (KW) statistical test [44] and p -value are computed.

Firstly, CRP method has been applied on the extracted IMF from the EEG signals and separately on the EEG signals without decomposition. The p -values of the features are depicted in Table 3.1.

Table 3.1: p -values of features extracted from EEG signals and from different IMFs by CRP method

Features	EEG signals	IMF1	IMF2	IMF3	IMF4	IMF5	IMF6	IMF7
RR	$2.3E - 8$	$5.2E - 6$	$5.5E - 6$	$7.1E - 4$	$6.2E - 4$	$4.8E - 4$	$5.1E - 3$	$5.5E - 2$
DET	$1.2E - 5$	$7.2E - 4$	$4.2E - 6$	$3.3E - 7$	$8.2E - 8$	$9.9E - 4$	$5.3E - 2$	$8.1E - 4$
ADL	$3.8E - 8$	$6.4E - 6$	$8.3E - 8$	$7.7E - 4$	$6.1E - 3$	$7.8E - 4$	$4.3E - 2$	$5.1E - 7$
ENT	$1.2E - 7$	$3.3E - 6$	$1.9E - 7$	$1.8E - 2$	$6.2E - 6$	$5.5E - 4$	$5.7E - 2$	$4.3E - 1$
TT	$4.1E - 7$	$1.8E - 5$	$7.3E - 4$	$1.5E - 7$	$1.8E - 4$	$1.9E - 4$	$7.8E - 2$	$5.1E - 2$
LAM	$4.2E - 4$	$1.5E - 7$	$1.8E - 4$	$1.7E - 6$	$1.5E - 6$	$7.3E - 4$	$8.3E - 7$	$5.4E - 2$
RT	$5.8E - 5$	$4.3E - 4$	$5.3E - 2$	$1.4E - 5$	$1.2E - 4$	$3.2E - 5$	$1.8E - 2$	$6.2E - 6$
RT2	$3.8E - 3$	$5.3E - 5$	$4.3E - 2$	$7.3E - 2$	$5.2E - 1$	$2.2E - 3$	$2.8E - 1$	$6.2E - 2$

Also, similar analysis has been carried out using JRP method. Table 3.2 shows the p -values of different features for different IMFs and EEG signals.

Table 3.2: p -values of features extracted from EEG signals and from different IMFs by JRP method

Features	EEG signals	IMF1	IMF2	IMF3	IMF4	IMF5	IMF6	IMF7
RR	$5.4E - 6$	$1.2E - 6$	$5.5E - 4$	$1.5E - 6$	$6.2E - 3$	$2.2E - 2$	$1.3E - 3$	$4.2E - 1$
DET	$1.1E - 6$	$1.8E - 7$	$3.2E - 5$	$3.1E - 5$	$4.1E - 4$	$8.8E - 4$	$7.5E - 2$	$2.2E - 2$
ADL	$2.3E - 7$	$2.3E - 5$	$4.1E - 4$	$7.8E - 5$	$4.1E - 4$	$7.2E - 2$	$1.2E - 1$	$1.2E - 2$
ENT	$1.8E - 3$	$3.4E - 4$	$4.1E - 5$	$7.1E - 5$	$5.6E - 4$	$3.5E - 1$	$4.5E - 2$	$5.2E - 1$
TT	$3.3E - 4$	$5.1E - 5$	$6.4E - 4$	$7.2E - 5$	$3.2E - 7$	$4.8E - 3$	$2.2E - 4$	$8.5E - 7$
LAM	$1.8E - 5$	$2.3E - 8$	$2.3E - 5$	$8.3E - 5$	$4.2E - 2$	$2.2E - 5$	$2.8E - 1$	$5.2E - 3$
RT	$2.8E - 6$	$2.1E - 3$	$1.3E - 5$	$8.3E - 2$	$7.2E - 4$	$3.2E - 5$	$4.8E - 2$	$5.4E - 2$
RT2	$7.8E - 5$	$8.3E - 4$	$4.3E - 4$	$6.3E - 5$	$2.2E - 2$	$4.2E - 4$	$3.8E - 1$	$1.2E - 3$

Moreover, the above two methods are studied simultaneously so as to understand the difference in the classification performance for both methods. Table 3.3 shows the comparison in terms of classification accuracy for the features obtained using CRP and JRP methods. We apply these methods on EEG signals and on the different modes obtained using the EMD method. The performance of LS-SVM classifier is measured in terms of classification accuracy where accuracy of the classifier is defined the ratio of number of correctly classified samples to the total number of samples. For finding the performance of the classifier, a cross-validation procedure with ten-fold has been used and Wilcoxon test [41, 11], Bhattacharya test [42, 11] and receiver operating characteristics (ROC) test [43, 11] are used for the ranking the different features.

Table 3.3: Comparison of classification accuracy of CRP and JRP methods

Input Signal	Ranking Method	Feature Index (CRP)	Max Acc (%) (CRP)	Feature Index (JRP)	Max Acc (%) (JRP)
EEG signals	ROC test	7,5,1	82	5,7,2	75
	Wilcoxon test	2,5,7	86	3,6,5	81
	Bhattacharya test	3,7,2	84	3,2,5	83
IMF1	ROC test	2,6,1	78	8,2,7,5	75
	Wilcoxon test	5,4,1	73	4,8,7	72
	Bhattacharya test	2,6,4,1	71	6,4,2	71
IMF2	ROC test	3,4,5	71	4,3,2	70
	Wilcoxon test	2,8,7	70	3,5,1	69
	Bhattacharya test	4,7,8	74	5,2,3	71
IMF3	ROC test	8,7,2	68	8,7	65
	Wilcoxon test	1,6,2	71	6,4,2	73
	Bhattacharya test	2,3,4	69	5,8,3	68
IMF4	ROC test	4,5,2	68	6,4	72
	Wilcoxon test	3,8,4	71	4,3,5	73
	Bhattacharya test	5,2,8	72	4,3,1	69

IMF5	ROC test	4,1,5	68	1,4,3	63
	Wilcoxon test	7,8,5	70	2,4,7	72
	Bhattacharya test	6,4,3	73	5,2,1	74
IMF6	ROC test	4,5,7	66	7,3,2	64
	Wilcoxon test	1,2,7	63	4,5,3,2	65
	Bhattacharya test	2,3,8	67	2,3,4,5	68
IMF7	ROC test	1,5,4	63	5,7,1	58
	Wilcoxon test	7,5,2	66	2,6,3	59
	Bhattacharya test	2,3,5	64	1,3,5,8	57

The features used in the classification are indexed in the order as: RR, DET, ADL, LAM, ENTR, RT, TT, RT2.

From Table 3.3, it has been observed that CRP parameters of EEG signals gives better classification accuracy. It means that CRP parameters are more significant than JRP parameters. Figures 3.1 and Figure 3.2 show the Box plots for CRP parameters and JRP parameters respectively for without decomposition and Figures 3.3 and 3.4 show the box plots for CRP and JRP parameters for IMF1 respectively.

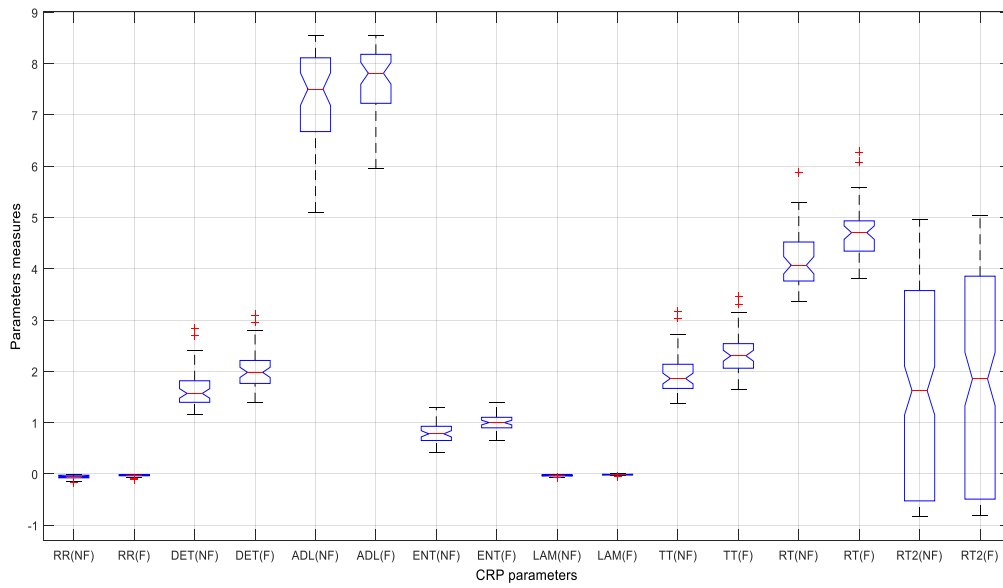


Figure 3.1: Box plots for CRP parameters for without decomposition

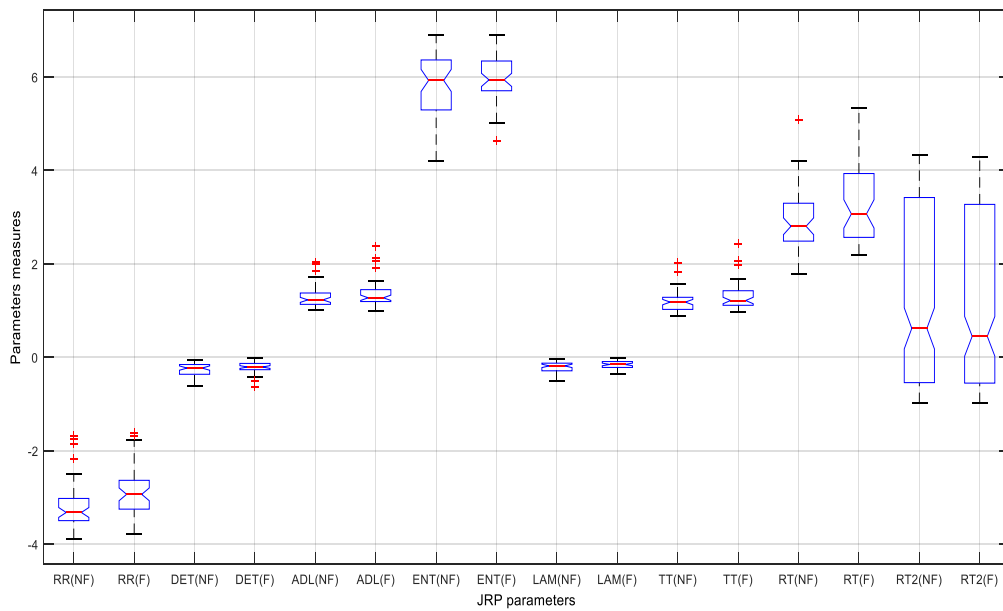


Figure 3.2: Box plots for JRP parameters for without decomposition

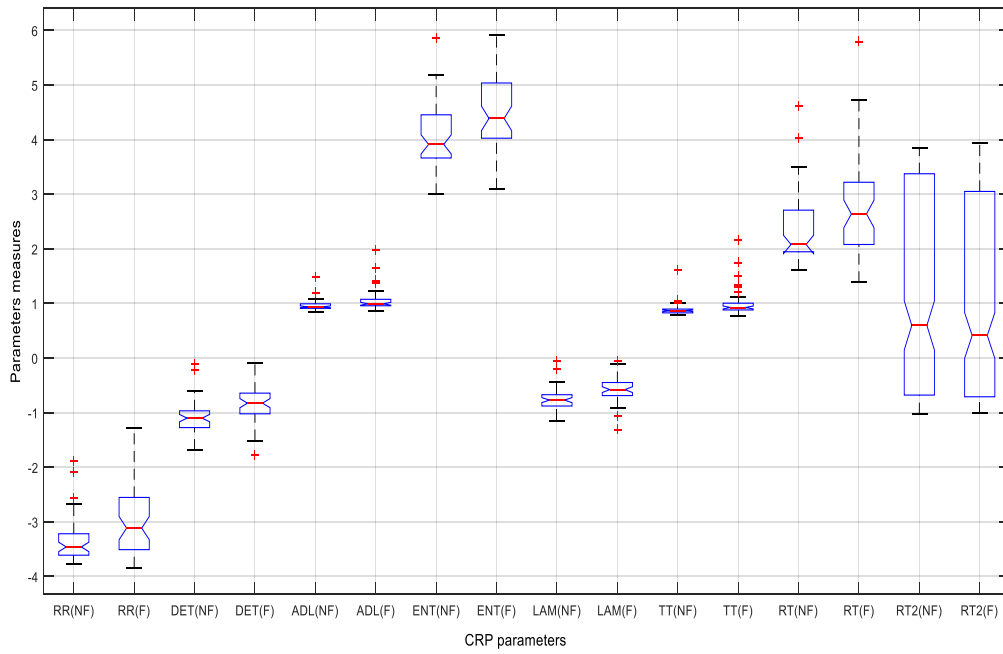


Figure 3.3: Box plots for CRP parameters of IMF1

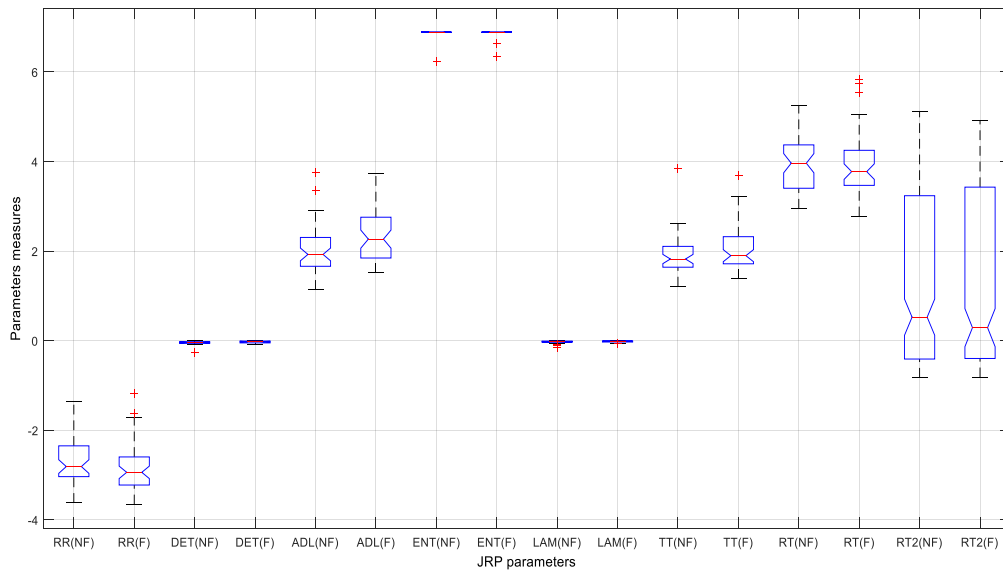


Figure 3.4: Box plots for JRP parameters of IMF1

3.2 Discussion

Basically, the entire study has been carried out to explore the CRP and JRP methods for classification of focal and non-focal EEG signals with and without EMD methods. Since, the nature of EEG signals is nonlinear and non-stationary. Therefore, the nonlinear methods can better extract information from EEG signals and consequently, they can give more accurate results.

In addition to this, a comparison is being performed between our proposed method and the existing automated methods that work on same database and it is presented in Table 3.4.

Table 3.4: Comparison of classification accuracy obtained from the different classification methods

Authors	Data set	Features	Classification accuracy (%)
Zhu et al. [45]	50 signals	DPE	84
	750 signal		75
Sharma et al.[10]	50 signals	AVIF and ASE	85
Sharma et al.[12]	50 signals	Entropies	87
Present work	50 signals	CRP and JRP parameters	86

Authors in [45] have analysed the two subsets of 50 and 750 pairs of EEG signals for both focal as well as non-focal EEG classes. Among all the channel recordings, single-channel recordings are utilized for classification of S_{focal} and $S_{nonfocal}$ EEG signals. The techniques used for classification is delay permutation entropy (DPE) [45]. The classification

performed has accuracies of about 84% and 75% for both the sets of 50 and 750 EEG signals respectively.

Authors in [10] have done classification only for the first 50 sets of S_{focal} and $S_{nonfocal}$ EEG signals. The features that are used for classification are average variance of instantaneous frequencies (AVIF) and average sample entropy (ASE) of IMFs of S_{focal} and $S_{nonfocal}$ EEG signals. The accuracy obtained in this case is 85% with the help of LS-SVM classifier. Authors in [12] evaluated the entropy features from the IMFs of S_{focal} and $S_{nonfocal}$ EEG signals. Some entropies that are used for classification are Renyi, average Shannon, approximate, and phase entropies. The accuracy obtained is 87% when the above average entropies are implemented with LS-SVM classifier.

Here, CRP and JRP parameters are used for extracting parameters from S_{focal} and $S_{nonfocal}$ EEG signals. In order to find suitable parameters, classification accuracy has been evaluated using LS-SVM classifier. Highest classification accuracy which is 86% obtained using determinism, entropy and trapping time features extracted from CRP.

The Kruskal-Wallis test is used to quantitatively analyse the discrimination ability of each feature. This test gives a parameter known as p -value which measures the similarity between two different classes. Significant features are shown in Table 3.1 and Table 3.2 with $p \leq 0.05$.

Chapter 4

Conclusions and Future Work

In this chapter, conclusions and future scope related to this research work have been provided.

4.1 Conclusions

In this work, a new method has been proposed that is based on RP to automatically classify the EEG signals. The features that are extracted from IMFs are developed and used to classify focal and non-focal EEG signals.

The LS-SVM together with radial basis function kernel has given the maximum classification accuracy for EEG signals and its value is 86%. In this method, the trial and error method is applied to select the kernel parameters. In future, it would be of great interest to implement a strategy that can automatically select the kernel parameters and kernel function. The proposed method for classification of non-focal and focal EEG signals has been studied and observed on very limited database. Therefore, it is necessary to study the above method on a larger database before applying it for medical purposes.

4.2 Scope for future work

This methodology can be studied for multi-variate signals wherein EEG signals of brain affected with other disease can be considered as bivariate. Further performance of the proposed methodology can be validated on larger databases. In addition, this methodology can be studied on signals of other parts of the body, e.g. heart, muscles etc.

It would be of interest to study the effect of window size on the classification accuracy in the classification of focal and non-focal EEG signals. In future other non-stationary signal decompositions based methods can be studied for extraction of features for classification of focal and non-focal EEG signals.

References

- [1] S. Pati and A.V. Alexopoulos, “Pharmacoresistant epilepsy: From pathogenesis to current and emerging therapies,” *Cleveland Clinic Journal of Medicine*, vol. 77, no. 7, pp. 457-467, 2010.
- [2] G.D. Cascino, “Surgical treatment for extratemporal epilepsy,” *Current Treatment in Options in Neurology*, vol. 6, pp. 257-262, 2004.
- [3] A. Awad, J. Rosenfeld, J. Ahl, J.F. Hahn and H. Lüders, “Intractable epilepsy and structural lesions of the brain: mapping, resection strategies, and seizure outcome,” *Epilepsia*, vol. 32, pp. 179–186, 1991.
- [4] World Health Organisation: Epilepsy. <http://www.who.int/mediacentre/factsheets/fs999/en/> Access Date: 07/04/2016.
- [5] Epilepsy Health Centre: Types of epilepsy. www.webmd.com/epilepsy/guide/types-epilepsy Access Date: 07/04/2016.
- [6] U.R. Acharya, O. Faustand, N. Kannathal, T.L. Chua and S. Laxminarayan , “Non-linear analysis of EEG signals at various sleep stages,” *Computer Methods and Programs in Biomedicine*, vol. 80, no. 1, pp. 37–45, 2015.
- [7] T.S. Kumar, V. Kanhangad and R.B. Pachori, “Classification of seizure and seizure- free EEG signals using multi-level local patterns,” *IEEE 19th International Conference on Digital Signal Processing*, pp. 646-650, 2014.
- [8] U.R. Acharya, C.K. Chua, T.C. Lim, J.S. Dorithy and Suri, “Automatic identification of epileptic EEG signals using nonlinear parameters,” *Journal of Mechanics in Medicine and Biology*, vol. 9, pp. 539–553, 2009.

- [9] R.G. Andrzejak, K. Schindler and C. Rummel, “Nonrandomness, nonlinear dependence, and nonstationarity of electroencephalographic recordings from epilepsy patients,” *Physical Review E*, vol. 86, 046206, 2012.
- [10] R. Sharma and R.B. Pachori, “Empirical mode decomposition based classification of focal and non-focal EEG signals,” *International Conference on Medical Biometrics*, 2014.
- [11] R. Sharma, R.B. Pachori and U.R. Acharya, “An integrated index for the identification of focal electroencephalogram signals using discrete wavelet transform and entropy measures,” *Entropy*, vol. 17, pp. 5218-5240, 2015.
- [12] R. Sharma, R.B. Pachori and U.R. Acharya, “Application of entropy measures on intrinsic mode functions for automated identification of focal electroencephalogram signals,” *Entropy*, vol.17, pp. 669-691, 2015.
- [13] L. Guo, D. Rivero and A. Pazos, “Epileptic seizure detection using multiwavelet transform based approximate entropy and artificial neural networks,” *Journal of Neuroscience Methods*, vol. 193, no. 1, pp. 156- 163, 2010.
- [14] J. Lamberts, P.L.C. Van den Broek, J. Bener, J. Van Egmond, R. Dirksen and A.M.L. Cohen, “Correlation dimension of the human electroencephalogram corresponding to cognitive load,” *Neuropsychobiology*, vol. 41, no. 3, pp. 149–153, 2000.
- [15] G.J Ortega, L. Menendez de la Prida, R.G. Sola and J. Pastor, “Synchronization clusters of interictal activity in the lateral temporal cortex of epileptic patients: Intraoperative electrocorticographic analysis,” *Epilepsia*, vol.49, pp.269–280, 2008.
- [16] V.L. Towle, R.K. Carder, L. Khorasani and D. Lindberg, “Electrocorticographic coherence patterns,” *Journal of Clinical Neurophysiology*, vol. 16, pp. 528-547, 1999.

- [17] P.V. Mierlo, E. Carrette, H. Halle, R. Raedt, and A. Meurs, "Ictal-onset localization through connectivity analysis of intracranial EEG signals in patients with refractory epilepsy," *Epilepsia*, vol. 54, pp. 1409-1418, 2013.
- [18] K. Lehnertz, C.E. Elger, "Spatio-temporal dynamics of the primary epileptogenic area in temporal lobe epilepsy characterized by neuronal complexity loss," *Electroencephalography and clinical neurophysiology*, vol. 95, pp. 108-117, 1995.
- [19] N.E. Huang, et al., "The empirical mode decomposition and the Hilbert spectrum for nonlinear and non-stationary time series analysis," *Proceedings of the Royal Society of London. Series A: Mathematical, Physical and Engineering Sciences*, vol. 454, no. 1971, pp. 903–995, 1998.
- [20] V. Bajaj and R.B. Pachori, "EEG signal classification using empirical mode decomposition and support vector machine," *Proceedings International Conference on Soft Computing for Problem Solving*, pp. 623-635, 2011.
- [21] R.B. Pachori and V. Bajaj, "Analysis of normal and epileptic seizure EEG signals using empirical mode decomposition," *Computer Methods and Programs in Biomedicine*, vol. 104, no. 3, pp. 373–381, 2011.
- [22] N. Marwan, M. Carmen Romano, M. Thiel and J. Kurths, "Recurrence plots for the analysis of complex systems," *Physics Reports*, vol. 438, pp. 237–329, 2007.
- [23] J.A.K. Sukens and J. Vandewalle, "Least squares support vector machine classifiers," *Neural Processing Letters*, vol. 9, no. 3, pp. 293-300, 1999.

- [24] V. Bajaj and R.B. Pachori, "Classification of seizure and nonseizure EEG signals using empirical mode decomposition," *IEEE Transactions on Information Technology in Biomedicine*, vol. 16, no. 6, pp. 1135–1142, 2012.
- [25] R.B. Pachori, "Discrimination between ictal and seizure-free EEG signals using empirical mode decomposition," *Research Letters in Signal Processing*, vol. 2008, pp. 1-5, 2008.
- [26] V. Bajaj and R.B. Pachori, "Epileptic seizure detection based on the instantaneous area of analytic intrinsic mode functions of EEG signals," *Biomedical Engineering Letters*, vol. 3, no. 1, pp.17–21, 2013.
- [27] J.P. Zbilut, M. Koebbe, H. Loeb and G. Mayer-Kress, "Use of recurrence plots in the analysis of heart beat intervals," *Proceedings of the IEEE Conference on Computers in Cardiology*, pp. 263–266, 1991.
- [28] N. Marwan, N. Wessel, U. Meyerfeldt, A. Schirdewan and J. Kurths, "Recurrence plot based measures of complexity and its application to heart rate variability data," *Physical Review E*, vol. 66, no. 2, 2002.
- [29] F. Takens, "Detecting Strange Attractors in Turbulence," *Springer*, pp. 366, 1981.
- [30] H. Kantz and T. Schreiber, "Nonlinear Time Series Analysis," *Cambridge University Press*, pp.30, 1997.
- [31] N. Marwan and J. Kurths, "Nonlinear analysis of bivariate data with cross recurrence plots," *Physics Letters A*, vol. 302, pp. 299–307, 2002.
- [32] N. Marwan, M. Thiel and N.R. Nowaczyk, "Cross recurrence plot based synchronization of time series," *Nonlinear Processes in Geophysics*, vol. 9, pp. 325–331, 2002.

- [33] A. Fabretti and M. Ausloos, "Recurrence plot and recurrence quantification analysis techniques for detecting a critical regime. Examples from financial market indices," *International Journal of Modern Physics C*, vol. 16, pp. 671–706, 2005.
- [34] M. Thiel, M.C. Romano, J. Kurths, R. Meucci, E. Allaria and F.T. Arecchi, "Influence of observational noise on the recurrence quantification analysis," *Physica D: Nonlinear Phenomena*, vol. 171, pp. 138–152, 2002.
- [35] L.L. Trulla, A. Giuliani, J.P. Zbilut and C.L. Webber, "Recurrence quantification analysis of the logistic equation with transients," *Physics Letters A*, vol. 223, pp. 255–260, 1996.
- [36] V.N Vapnik, "The Nature of Statistical Learning Theory," *IEEE Transactions on Neural Networks*, vol. 10, 2000.
- [37] J.A.K. Sukens and J. Vandewalle, "Least squares support vector machine classifiers," *Neural Processing Letters*, vol. 9, no. 3, pp. 293-300, 1999.
- [38] C. Cortes and V. Vapnik, "Support-vector networks," *Machine Learning*, vol. 20, no. 3, pp. 273–297, 1995.
- [39] A.H. Khandoker, D.T.H. Lai, R.K. Begg, M. Palaniswami, "Wavelet-based feature extraction for support vector machines for screening balance impairments in the elderly," *IEEE Transactions on Neural Systems and Rehabilitation Engineering*, vol. 15, no. 4, pp. 587–597, 2007.
- [40] M. Zavar, S. Rahati, M.R. Akbarzadeh-T and H. Ghasemifard, "Evolutionary model selection in a wavelet-based support vector machine for automated seizure detection," *Expert Systems with Applications*, vol. 38, pp.10751–10758, 2011.

- [41] R. Bergmann, J. Ludbrook, Spooren and W.P.J.M, “Different outcomes of the Wilcoxon-Mann-Whitney test from different statistics packages,” *The American Statistician*, vol. 54, pp. 72–77, 2000.
- [42] T.Kailath, “The divergence and Bhattacharyya distance measures in signal selection,” *IEEE Transactions on Communication Technology*, vol. 15, pp. 52–60, 1967.
- [43] S. Theodoridis, K. Koutroumbas, “Feature selection. In Pattern Recognition,” *Second edition; Academic Press: San Diego*, pp. 163–205, 2003.
- [44] R.J. Freund, W.J. Wilson and D.L. Mohr, “Statistical Methods,” *3rd edition Academic Press, Burlington, MA, USA*, 2010.
- [45] G. Zhu, Y. Li, P. P. Wen, S. Wang, M. Xi, “Epileptogenic focus detection in intracranial EEG based on delay permutation entropy,” *Conference Proceedings, American Institute of Physics*, vol. 1559, pp. 31–36, 2013.